

# 行政院國家科學委員會專題研究計畫 成果報告

## 臺灣河口與沿岸海洋清除作用研究：延續計畫 研究成果報告(精簡版)

計畫類別：個別型  
計畫編號：NSC 95-2611-M-002-012-  
執行期間：95年08月01日至96年07月31日  
執行單位：國立臺灣大學海洋研究所

計畫主持人：魏慶琳

計畫參與人員：碩士班研究生-兼任助理：侯彥睿、林筱雨、蔡靜如

處理方式：本計畫可公開查詢

中華民國 96年08月15日

**Scavenging Phenomenon Elucidated by  $^{234}\text{Th}/^{238}\text{U}$  Disequilibria in the  
Surface Water of the Taiwan Strait**

Ching-Ling Wei, Jing-Ru Tsai, Yen-Ruei Hou, Liang-Saw Wen and Su-Cheng Pai

Institute of Oceanography  
National Taiwan University  
PO Box 23-13, Taipei 106  
Taiwan

## **Abstract**

Surface concentrations of dissolved (DTh) and particulate (PTh)  $^{234}\text{Th}$  at 38 stations in the Taiwan Strait were measured in May 2005. The spatial distribution of  $^{234}\text{Th}$  in the Taiwan Strait is controlled by the advective input of Kuroshio Branch Water via the Peng-Hu Channel and fast removal due to the high input of riverine particulates of the Cho-Sui River. A scavenging model with the physical transport component was applied to the DTh and PTh to estimate scavenging (J) and removal (P) fluxes of  $^{234}\text{Th}$ . The J flux ranges from 57 dpm/m<sup>3</sup>/d to 520 dpm/m<sup>3</sup>/d and the P flux ranges from 24 to 381 dpm/m<sup>3</sup>/d, respectively. Using  $^{234}\text{Th}$  as a proxy of particulate organic carbon, the removal rate of POC from the surface water of the Taiwan Strait ranges from  $0.6\pm 0.8$  in the Taiwan Bank to  $6.9\pm 3.5$  mmol/m<sup>3</sup>/d in the central Taiwan Strait.

## **Introduction**

As a result of complicated environmental settings, the study of biogeochemical processes in coastal environments is a challenging task for marine scientists. The complexity of coastal systems is mainly due to strong and variable physical forces and the significant input of allochthonous materials from the land. The Taiwan Strait is a shallow shelf with an average depth of 60 m and serves as an important conduit for water exchange between the South China Sea and the East China Sea (Fig. 1). A large northward volume transport of 2.0~2.2 Sv was measured by Chung et al. (2001) and the transport is mainly through the Peng-Hu Channel (Jan and Chao, 2003; Liang et al., 2002). Since this shallow and narrow water mass is bordered by the heavily populated coastline of China and Taiwan, the Taiwan Strait receives large amounts of anthropogenic contaminants discharged from municipal areas through river inputs.

While seawater is fed from the south, it is conceivable that the fluvial sediments contributed from the rivers on both sides of the Taiwan Strait not only serve as an important source of terrestrial materials on the one hand, but also act as an efficient scavenger and carrier for these elements. The combination of seismic activity and frequent typhoons results in extremely high sediment input from mountainous river systems in Taiwan. A total of 194 Mt/y fluvial sediments are carried into the Taiwan Strait by the western Taiwan river systems (Dadson et al., 2003). In order to understand the fate of elements either brought in from the south by through flow or discharged from the land into the Taiwan Strait, it is essential to obtain the rate of processes governing the budget of elements of interest. By applying suitable naturally occurring radionuclides, knowledge of rate information governing elemental cycling in the ocean can be obtained. Among those radionuclides, the short-lived  $^{234}\text{Th}$  ( $t_{1/2}=24.1$  d) is an ideal tool to address this information.

Produced constantly from  $^{238}\text{U}$  in seawater,  $^{234}\text{Th}$  is adsorbed quickly to particle surface and removed from the water column. Depending on how fast  $^{234}\text{Th}$  is removed from a given parcel of seawater; its degree of deviation from secular equilibrium activity varies in different regimes of the ocean. Used as a particle tracer,  $^{234}\text{Th}/^{238}\text{U}$  disequilibrium is suitable for the investigation of scavenging and removal processes on a time scale of days to weeks. Th-234 has been widely used as a proxy of particulate organic carbon (Murray et al., 1989; Buesseler et al., 2006), particulate inorganic carbon (Bacon et al., 1996), organic pollutants (Gustafsson et al., 1997), and trace metals (Weinstein and Moran, 200) to investigate elemental removal processes in the upper water column of the open oceans. However, due to the dynamic nature of coastal environments, there have been few studies applying the  $^{234}\text{Th}/^{238}\text{U}$  disequilibrium in coastal oceans (Wei and Murray, 1992; Gustafsson et al., 1998;

Benitez-Nelson et al., 2000; Radakovitch et al., 2003). No investigation of scavenging processes has been conducted in the Taiwan Strait.

In May 2006, we took the opportunity to join the Joint Hydrographic Survey launched by the National Center for Oceanographic Research of Taiwan (NCOR Report, 2006) to carry out aerial sampling in the Taiwan Strait for  $^{234}\text{Th}$  analyses. This expedition gave us the precious opportunity to take large-volume seawater samples covering the whole area of the Taiwan Strait and its fringe regions. This paper is aimed at providing a quantitative estimate of scavenging and removal rates by using the  $^{234}\text{Th}/^{238}\text{U}$  disequilibrium.

## **Methods**

At the stations shown in Figure 1, large-volume seawaters were sampled over the period of 21-27 May 2006 from the Joint Hydrographic Survey project (NCOR 2006) aboard three research vessels, the R/V Ocean Researcher 1 (cruise #796), the R/V Ocean Researcher 2 (cruise #1353), and the R/V Ocean Researcher 3 (cruise #1153). Seawater was collected at a depth of 2 meters using 10 L or 20 L Teflon-coated Go-Flo bottles mounted on a Sea-Bird CTD (SBE 9/11) rosette assembly. A total of 27 large-volume (20 L) surface seawater samples were collected for the determination of dissolved (DTh), particulate (PTh)  $^{234}\text{Th}$  and auxiliary hydrographic parameters (nutrients, particulate organic carbon and nitrogen).

### *Fluorescence and light transmission*

Along the cruise track, continuous measurements of fluorescence and transmission were measured by attaching a fluorometer and a transmissometer with a 25 cm light path length, respectively on the underway system (Wetlabs C-Star)

installed onboard. The intake of the underway system is about 2 meters below the surface.

#### *Particulate organic carbon and nitrogen*

Seawater for particulate organic carbon and nitrogen was filtered through a pre-combusted (450°C) Whatman 25 mm GF/F filter, wrapped in aluminum foil and stored at -4°C. In the laboratory, the filter was acid-fumed to remove carbonates and then measured with a Fisons elemental analyzer (NA1500).

#### *Dissolved <sup>234</sup>Th*

Immediately after the seawater was transferred to the pressure drums, compressed air (at 12 p.s.i.) was used to pressure filter the seawater through preweighed 142 mm Nuclepore filters (0.45 µm pore size) mounted in a Plexiglas filter holder. The filters were rinsed with approximately 15 ml deionized distilled water to remove sea salt and stored in a petri dish to determine the total suspended matter (TSM) concentration and particulate <sup>234</sup>Th activities.

The filtrate was acidified with about 20 ml of concentrated HCl and spiked with 30 dpm of <sup>230</sup>Th and 50 mg of Fe carrier. The samples were bubbled vigorously for at least 3 hours to help isotopic equilibration. Concentrated NaOH was then added to raise the pH~8 to precipitate Fe(OH)<sub>3</sub>. The Fe (OH)<sub>3</sub> precipitates, with adsorbed thorium, were collected by siphoning, centrifuging, and then dissolving in concentrated HCl to make the samples 9 N HCl. These samples were then passed through an anion exchange column (Dowex 1X-8) preconditioned by 9N HCl to separate uranium from thorium. Thorium samples were purified by passing the sample through three anion exchange columns pre-conditioned with 8 N HNO<sub>3</sub>. The sample

was evaporated down to one drop and was ready for extraction. Th-234 and the yield tracer,  $^{230}\text{Th}$ , were extracted into a 0.4 M TTA (thenoyltrifluoroacetone)-benzene solution and stippled on a stainless-steel disc. Preconcentration and separation of uranium and thorium from the filtered seawater samples were completed in three days after the samples were collected.

#### *TSM and particulate $^{234}\text{Th}$*

After weighing for the determination of TSM concentration, the filters were decomposed in the laboratory by soaking in  $\sim 10$  ml of concentrated  $\text{NH}_4\text{OH}$ . The samples were gently heated to evaporate the  $\text{NH}_4\text{OH}$  then fluxed in  $\text{HClO}_4/\text{HF}$  to thoroughly digest organic and inorganic materials. After digestion, the samples were purified and mounted on stainless-steel discs following the same procedures as for dissolved  $^{234}\text{Th}$  samples.

The activities of  $^{234}\text{Th}$  were counted by a low background ( $< 0.15$  cpm) anticoincidence counter (Riso GM25-5) via its  $\beta$ -emitting daughter  $^{234}\text{Pa}$ . Chemical yield of thorium was estimated by counting spiked  $^{230}\text{Th}$  using silicon surface-barrier detectors (EG&G Ortec 576). The counting efficiencies of the  $\alpha$  detectors were calibrated against NIST traceable  $^{230}\text{Th}$  (Isotope Products Laboratory 387-67-3) standard plates. Activities of  $^{234}\text{Th}$  reported here were corrected back to the sampling time after the ingrowth of  $^{234}\text{Th}$  from  $^{238}\text{U}$  was subtracted.

## **Results**

All data obtained from the bottle samples are listed in Table 1. Parameters are shown as contour maps.

The surface distributions of temperature and salinity are shown in Figures 2 and 3, respectively. The distributions of temperature and salinity reveal the hydrographic domains of the three water masses, the China Coastal Water (CCW), the Kuroshio Branch Water (KBW), and the South China Sea Surface Water (SCSSW). Generally, the hydrography in the Taiwan Strait is controlled by the interaction of CCW originating from the north with either KBW or the SCSSW from the south. Due to persistent northward currents in the Taiwan Strait, the CCW, which is characterized by low temperature and salinity, is limited to the northwestern Taiwan Strait. Significant freshening shown in the salinity distribution in the northwestern Taiwan Strait is evidently caused by the influence of the river input from the coast of China. The KBW with high temperature and salinity dominates the southeastern part of the Taiwan Strait and reaches as far north as to 24°30'N in the coastal region of western Taiwan. With intermediate temperature and salinity values, the SCSSW occupies most part of the Taiwan Strait. Shown in Figure 1, a strong and persistent current from the northeastern South China Sea through the Peng-Hu Channel is identified (Jan and Chao, 2003). Chung et al. (2001) concluded that the water mass in this northward current originated from the KBW in May and from the South China Sea Warm Water in August.

The surface distributions of fluorescence expressed as relative fluorescence unit (RFU) and light beam attenuation coefficient are shown in Figures 4 and 5. The distribution of fluorescence generally reflects the geographic distribution of chlorophyll concentration. The RFU in the surface water shows a higher value in the western and northern portions of the Taiwan Strait. Higher fluorescence water is associated with higher silicate concentration (data not shown). The distribution for fluorescence concurs with the total pigments measured by HPLC in the samples



collected from the same stations of this study (Tung, 2007). The highest and lowest biomasses are found in the Ming River mouth and Cho-Sui River mouth. Tung (2007) reported that the chlorophyll biomass is mostly contributed (>80%) by diatoms in the region of the Ming River and Cho-Lung River mouths.

The distribution of BAC essentially represents the geographical variability of TSM, which is shown in Figure 6. A good correlation between TSM and BAC was obtained,

$$\text{TSM (mg/L)} = 2.40 \times \text{BAC (1/m)} - 0.75, R^2=0.88, n=64.$$

In the vicinity of the Cho-Sui River mouth, the BAC is the highest, indicating the fluvial sediment input. It is noted that the BAC in the Ming River mouth showed elevated values, whereas the TSM distribution in this region remained low. Since the beam attenuation coefficient is also affected by colored dissolved substances (Zaneveld, 1994), elevated BAC in the vicinity of Ming River mouth may be caused by fluvial input of dissolved substances instead of being caused by absorption and scattering of particles. Indeed, Hung et al. (2000; 2003) observed a water mass of high dissolved organic carbon (> 90  $\mu\text{M}$ ) occupied the vicinity of the Ming River mouth. Not surprisingly, TSM concentration is higher in the vicinity of Cho-Sui River mouth and in the coastal water of China. Clearer water from the South China Sea dominated the southern Taiwan Strait.

POC distribution in the study region is shown in Figure 7. Generally, the POC concentration is higher in the western than in the eastern Taiwan Strait. It is evident that the POC concentration increases in the regions under the influence of riverine inputs. No POC data was measured south of 23°N, but the POC concentration ranges between 8.8 and 16.3  $\mu\text{M}$  were observed by Kao et al. (2006) in the surface water off southwestern Taiwan, indicating the POC concentration in the southern part of the

Taiwan Strait is in the same range of our POC level in the eastern side of Taiwan Strait.

Contours of dissolved DTh and PTh are shown in Figures 8 and 9. The spatial distribution of DTh corroborates with the circulation pattern in the Taiwan Strait. A relatively high DTh is associated with the KBC and extends northward through the Peng-Hu Channel. The DTh in the shallow shelf of the study area showed very low values ( $<0.5$  dpm/L). Unlike the DTh distribution, the PTh showed low values in the regions of the Ming River mouth and off the southwestern Taiwan coast. A patch of high PTh was found in the vicinity of the Cho-Sui River mouth.

## **Discussions**

Due to its highly particle-reactive characteristics,  $^{234}\text{Th}$  is rapidly removed from seawater to the extent that large deficiency from the secular equilibrium, especially in the shallow shelf region of the Taiwan Strait, was observed. The ratios of total (dissolved + particulate)  $^{234}\text{Th}$  at most of our sampling stations are lower than 0.4, indicating the particle removal rate is faster than the mixing rate of water in the Taiwan Strait.

Since the simple irreversible scavenging model was first used for estimating the scavenging and removal rates of  $^{234}\text{Th}$  in seawater (Coale and Bruland, 1985), the oceanography community has pled for a more realistic model for  $^{234}\text{Th}$  budgeting in the ocean. For budgeting  $^{234}\text{Th}$  in a dynamic environment, where advective transport may significantly control the  $^{234}\text{Th}$  distribution, it should also take into account the physical mixing term (Benitez-Nelson et al., 2000; Seyvor et al., 2006). Assuming a

steady state, the mass balance of DTh and PTh are described by the following equations.

$$\frac{dDTh_i}{dt} = 0 = \frac{V_{i-1}DTh_{i-1} - V_iDTh_i}{\Delta L} + \lambda U_i - \lambda DTh_i - J_i \quad (1)$$

$$\frac{dPTh_i}{dt} = 0 = J_i + \frac{V_{i-1}PTh_{i-1} - V_iPTh_i}{\Delta L} - \lambda PTh_i - R_i \quad (2)$$

Where

$U_i = {}^{238}\text{U}$  activity in i-th box (dpm/m<sup>3</sup>)

$DTh_i =$  dissolved  ${}^{234}\text{Th}$  activity in i-th box (dpm/m<sup>3</sup>)

$PTh_i =$  particulate  ${}^{234}\text{Th}$  activity in i-th box (dpm/m<sup>3</sup>)

$V_i =$  average current velocity of i-th box (m/d)

$\Delta L =$  length of box along the direction of average flow (m)

$\lambda =$  radioactive decay constant of  ${}^{234}\text{Th}$  (1/d)

$J_i =$  net change rate of dissolved  ${}^{234}\text{Th}$  due to scavenging process in i-th box  
(dpm/m<sup>3</sup>/d)

$R_i =$  net change rate of particulate  ${}^{234}\text{Th}$  due to particle removal process in i-th  
box (dpm/m<sup>3</sup>/d)

In the model, the particulate phase is assumed to be transported by the current, because fine particles remain in suspension in this dynamic system of strong advection. The residence times of dissolved ( $\tau_d$ ) and particulate ( $\tau_p$ )  ${}^{234}\text{Th}$  with respect to scavenging and particle removal rates, respectively, can be calculated by:

$$\tau_d = \frac{DTh}{J} \quad (3)$$

$$\tau_p = \frac{PTh}{R} \quad (4)$$

Based on the environmental settings and the spatial distribution of DTh and PTh, the study area was divided into five domains to carry out the advection-scavenging-removal model. Following the procedures of Liang et al. (2003),

mean current velocity in May at the boundary of each box was estimated by averaging archived shipboard ADCP data (NCOR Data Bank) collected during 1991~2006. In each box, the numbers of data sets for averaging current velocity range from 2400 to 3115, which gives a root mean square (rms) error of ~5 cm/s (Liang et al., 2003).

Average DTh and PTh, average values of current velocities, and results of advection-scavenging-removal model on dissolved and particulate  $^{234}\text{Th}$  for the five domains in the Taiwan Strait are shown in Table 2. The net changes due to physical transport, J and P, and residence times of DTh and PTh are shown in Figure 10. Since both ADCP and current meter data collected from the Luzon Strait showed that a persistent and strong Kuroshio Branch Water flow through the Northern Luzon Strait into the region of southwestern Taiwan (Liang et al., 2003), we used 1.3 and 0.2 dpm/L, respectively, as the DTh and PTh of influx water into Box I (Wei and Hung, 1992). The average DTh and PTh activities of the influx water of Box II were  $1.0 \pm 0.2$  dpm/L and  $0.2 \pm 0.04$  dpm/L, which were measured at the northern South China Sea (unpublished results).

Depending on the average current velocity and the differences of DTh and PTh between adjacent boxes, the contributions of physical transport process to the  $^{234}\text{Th}$  mass balance vary from -8 to 460 dpm/m<sup>3</sup>/d and from -15 to 57 dpm/m<sup>3</sup>/d for DTh and PTh, respectively. Positive values indicate more  $^{234}\text{Th}$  was brought into than carried out from the box, whereas negative values indicate the amount of  $^{234}\text{Th}$  brought into the box is less than that transported out. Not surprisingly, physical transport causes the largest effect on the  $^{234}\text{Th}$  budgeting in the central part of the Taiwan Strait (Box III and IV) because a large amount of dissolved  $^{234}\text{Th}$  was carried into the Taiwan Strait by the strong current through the Peng-Hu Channel (Figure 1).

It should be noted that the physical transport term for DTh in Box III exceeds the in situ  $^{234}\text{Th}$  production from  $^{238}\text{U}$  decay ( $\sim 70 \text{ dpm/m}^3/\text{d}$ ) by a factor of 6.

It can be seen that, although significant for Th budget in each box, net changes of DTh and PTh by physical transport are generally smaller than scavenging (J in equation (1)) and particle removal (P in equation (2)) rates. Concurring with the biochemical settings of each domain, the J ranges from  $57 \text{ dpm/m}^3/\text{d}$  in Box V to  $520 \text{ dpm/m}^3/\text{d}$  in Box III and the P ranges from  $24 \text{ dpm/m}^3/\text{d}$  in Box II to 381 in Box III.

Box I represents the only domain deeper than 200 m in the Taiwan Strait and shows the hydrographic characteristics of Kuroshio Branch Current. A scavenging rate of  $91 \text{ dpm/m}^3/\text{d}$  and particle removal rate of  $138 \text{ dpm/m}^3/\text{d}$  were obtained from the model calculation, which result in the residence times of 18 and 2 days for dissolved  $^{234}\text{Th}$  and particulate  $^{234}\text{Th}$ , respectively. The model results implies that  $^{234}\text{Th}$  cycling in this region is limited by the scavenging rate and, once scavenged onto the particles,  $^{234}\text{Th}$  is removed from the surface water in a very short period of time.

Box II encloses the Taiwan Bank, a shallow area of only 20 m average depth. It is noted that an eddy covering the Taiwan Bank (Figure 1) may enhance the suspension. The DTh and PTh data in Box II also showed a relatively homogeneous distribution, supporting the enhanced mixing due to the eddy. In contrast to the Box I, the J is larger than P, implying that the strong tidal forces inhibited particle settling. A relative long particulate  $^{234}\text{Th}$  residence time of 16 days was obtained.

Both the highest scavenging and removal rates calculated by the model were found in Box III. As shown in the DTh contour, northward transport of South China Sea water brings in large amount of  $^{234}\text{Th}$  through the Peng-Hu Channel. The role the Cho-Sui River plays can be seen from the PTh distribution, which is dramatically elevated around  $23^\circ\text{N}\sim 24^\circ\text{N}$  of the eastern Taiwan Strait. Large input of terrestrial

suspended materials brought in by the Cho-Sui River scavenges thorium from seawater to cause elevated PTh patch in the map. Among many rivers of western Taiwan, the Cho-Sui River has been known as a major fluvial sediment source of the Taiwan Strait. Annual sediment input of Cho-Sui River is 64 Mt, 70% of the total sediment transportation of the western Taiwan rivers (Dadson et al., 2003). This large fluvial input serves as an efficient interceptor for particle-reactive elements transported with the current from the south. High P value found in Box III is conceivably based on the fact of the fast settling of coarse sediments from the fluvial input of the Cho-Sui River. The residence times of dissolved and particulate  $^{234}\text{Th}$  with respect to the scavenging and removal rates are extremely short, one day.

Box V covers the region affected by Ming River input, in which both DTh and PTh are low (Figures 8 and 9). Among the five boxes, the scavenging rate in this domain is the lowest, 57 dpm/m<sup>3</sup>/d, and the particle removal rate is relatively low, 76 dpm/m<sup>3</sup>/d. The Low J is attributed to the high concentration of dissolved organic matter in the region. Hung et al. (2000) observed that a high concentration (80~119  $\mu\text{M}$ ) of DOC, of which ~27% is in the colloidal form (>1 kDa), in the region near the Ming River. High dissolved organic materials provide more complexing ligands for retaining thorium in the dissolved phase.

Here we use  $^{234}\text{Th}$  as a proxy of organic carbon to approximate the removal rate of POC via particle settling in the Taiwan Strait. The removal rates of POC ( $P_c$ ) were calculated by  $P_{ix}$  ( $\text{POC}/\text{PTh}$ )<sub>i</sub>, where ( $\text{POC}/\text{PTh}$ )<sub>i</sub> is the ratio of particulate organic carbon and particulate  $^{234}\text{Th}$  for box i. The ( $\text{POC}/\text{PTh}$ )<sub>i</sub>, an important parameter of using  $^{234}\text{Th}$  as the carbon tracer for estimating carbon export, shows a large range of variation in the Taiwan Strait, ranging between 8 to 154  $\mu\text{mol}/\text{dpm}$  (Figure 11). Benitez-Nelson et al. (2000) also observed a large range of POC/PTh ratio, from 5 to

113  $\mu\text{mol/dpm}$ , in filtered particles collected from the surface water of the Gulf of Maine. Bueseller et al. (2006) gave a thorough discussion of the factors that may attribute to the variability of POC/PTh ratio in particles, including size, composition, shape, morphology, and sinking velocity of particles. Biogeochemical settings are responsible for the high variability of POC/PTh ratio in the Taiwan Strait. Specific concentration of organic carbon in the suspended particles shows higher organic-rich particles along the China coast, which may be caused by enhanced growth of biological particles induced from terrestrial input of nutrients. It was noted that the biomass in the domain covered by Box V is dominated by diatoms (Tung, 2007). The highest POC/PTh in northwestern Taiwan Strait can reach a value as high as 154  $\mu\text{mol/dpm}$  and implies that planktons grown in the region should be larger in size. These carbon-enriched meso- to macroplanktons, with smaller surface to volume ratios, provide fewer sites for thorium scavenging. On the contrary, in the southern Taiwan Strait, POC/PTh is much lower, which implies that planktons residing in the South China Sea seawater are smaller in size due to its oligotrophic setting of the water mass. Indeed, Tung (2007) found the dominant planktons are cyanobacteria in this region. The lowest POC/PTh was found in Box III, the region under the influence of the Cho-Sui River, which brought in large amounts of detritus materials containing less organic carbon and resulting in low POC/PTh.

The average POC/PTh ratio, the POC removal rate and the residence time of POC with respect to the POC removal rate ( $\tau_c$ ) in five domains of the Taiwan Strait are shown in Table 2. The removal rate of POC from the surface water of the Taiwan Strait ranges from 0.6~6.9  $\text{mmol/m}^3/\text{d}$ . Generally, the POC removal rate in the southern Taiwan Strait is lower than that in the northern Taiwan Strait. The lowest POC removal rate was in the Taiwan Bank, which may be a result of resuspension in

this shallow region. With respect to the removal rate, the residence time of POC in the Taiwan Strait ranges from 1 day in Box III to 17 days in Box II. The POC residence time with respect to particle removal rate in Box V is  $3\pm 3$  days. This estimate of POC residence time was comparable with Hung et al. (2000), which gave a residence time of 6 days for POC estimated from the quotient of the POC inventory in the euphotic layer and the new production rate in the inner shelf of the southern East China Sea, the region immediately to the north of our Box V.

## Conclusions

Aerial distributions of dissolved and particulate  $^{234}\text{Th}$  were determined to provide a quantitative estimate of the scavenging and particle removal rates in the surface water of the Taiwan Strait. By multiplying the ratio of POC/PTh ratio by the particle removal rate estimated from  $^{234}\text{Th}/^{238}\text{U}$  disequilibria, the removal rate of particulate organic carbon from the surface water of the Taiwan Strait was also estimated. Based on the environmental settings and  $^{234}\text{Th}$  scavenging/removal rates, five domains in the Taiwan Strait can be identified:

- (1) The Kuroshio Branch Water, where high temperature and salinity are found. The scavenging and removal rates of  $^{234}\text{Th}$  are similar to the open ocean with the  $\tau_d$  and  $\tau_p$  of 18 and 2 days, respectively.
- (2) The Taiwan Bank, where the lowest scavenging and removal rates were found due to resuspension of bottom sediments in this shallow region. The removal rate of POC from the surface water in this region is the lowest,  $0.6\pm 0.8$  mmol/m<sup>3</sup>/d, among the five domains of the study area.



- (3) The Cho-Sui River mouth, where extremely high particle concentration was observed. The  $^{234}\text{Th}$  is scavenged and removed at a very fast rate with the  $\tau_d$  and  $\tau_p$  of one day only.
- (4) The middle Taiwan Strait, where the intermediate scavenging and particle removal rates were observed.
- (5) The Ming River mouth, where low temperature, low salinity and high chlorophyll-a were observed; in this region the  $\tau_d$  and  $\tau_p$  are 2 and 3 days, respectively.

### **Acknowledgements**

We acknowledge the NCOR Data Bank for providing us with valuable historical ADCP data. We thank Y.H. Wang for help with the ADCP data processing and H.S. Wang for underway data processing. Help was also provided by the crews from the R/Vs Ocean Researcher I, II, III, and was greatly appreciated. This research was supported by NSC-95-2611-M-002-012.

## Figure Captions

Figure 1. Bathymetric map with large-volume sampling stations of the Taiwan Strait.

Mean surface current calculated from the historical shipboard May ADCP data collected during 1991~2006 are shown as vectors.

Figure 2. Surface distributions of temperature

Figure 3. Surface distribution of salinity.

Figure 4. Surface distributions of relative fluorescence unit (RFU) measured by fluorometer attached to the underway system during the cruise.

Figure 5. Surface distributions of beam light attenuation coefficient (BAC) readings measured by transmissometer attached to the underway system during the cruise.

Figure 6. Surface distributions of total suspended matter (TSM) concentration.

Figure 7. Surface distributions of particulate organic carbon.

Figure 8. Surface distributions of dissolved  $^{234}\text{Th}$ .

Figure 9. Surface distributions of particulate  $^{234}\text{Th}$ .

Figure 10. Results of advection-scavenging-removal model on dissolved and particulate  $^{234}\text{Th}$  in the Taiwan Strait. Three sets of bar plots in each domains represent the net change due to physical transport, J and P terms of equations (1) and (2), and residence times for DTh (open bar) and PTh (filled bar), respectively. Rate terms are in unit of dpm/m<sup>3</sup>/d and residence times are in unit of day. Error bars are propagated errors from average current velocity and standard deviations of average DTh and PTh in each box.

Figure 11. Surface distributions of the ratio of particulate organic carbon and particulate  $^{234}\text{Th}$ , (POC/PTh).

## References

- Bacon, M. P., J. K. Cochran, D. Hirschberg, T. R. Hammar, A. P. Fleer, 1996. Export flux of carbon at the equator during the EqPac time-series cruises estimated from  $^{234}\text{Th}$  measurements. *Deep-Sea Research II*, **43**, 1133-1153.
- Benitez-Nelson, C., K. O. Buesseler, G. Crossin, 2000. Upper ocean carbon export, horizontal transport, and vertical eddy diffusivity in the southwestern Gulf of Maine. *Continental Shelf Research* **20**, 707-736.
- Buesseler, K. O., C. R. Benitez-Nelson, S. B. Moran, A. Burd, M. Charette, J. K. Cochran, L. Coppola, N. S. Fisher, S. W. Fowler, W. D. Gardner, L. D. Guo, O. Gustafsson, C. Lamborg, P. Masque, J. C. Miquel, U. Passow, P. H. Santschi, N. Savoye, G. Stewart, T. Trull, 2006. An assessment of particulate organic carbon to thorium-234 ratios in the ocean and their impact on the application of  $^{234}\text{Th}$  as a POC flux proxy. *Marine Chemistry* **100**, 213-233.
- Chung, S.-W., S. Jan, K.-K. Liu, 2001. Nutrient fluxes through the Taiwan Strait in Spring and Summer 1999. *Journal of Oceanography* **57**, 47-53.
- Coale, K. H., K. W. Bruland, 1985.  $^{234}\text{Th}$ : $^{238}\text{U}$  disequilibria within the California Current. *Limnology and Oceanography* **30**, 22-33.
- Dadson, S. J., N. Hovius, H. Chen, W. B. Dade, M. L. Hsieh, S. D. Willett, J. C. Hu, M. J. Horng, M. C. Chen, C. P. Stark, D. Lague, J. C. Lin, 2003. Links between erosion, runoff variability and seismicity in the Taiwan orogen. *Nature* **426**, 648-651.
- Gustafsson, O., P. M. Gschwend, K. O. Buesseler, 1997. Using Th-234 disequilibria to estimate the vertical removal rates of polycyclic aromatic hydrocarbons from the surface ocean. *Marine Chemistry* **57**, 11-23.

- Gustafsson, O., K. O. Buesseler, W. R. Geyer, S. B. Moran, P. M. Gschwend, 1998. An assessment of the relative importance of horizontal and vertical transport of particle-reactive chemicals in the coastal ocean. *Continental Shelf Research* **18**, 805-829.
- Hung, J.-J., P.-L. Lin, K.-K. Liu, 2000. Dissolved and particulate organic carbon in the southern East China Sea. *Continental Shelf Research* **20**, 545-569.
- Hung, J.-J., C.-H. Chen, G.-C. Gong, D.-D. Sheu, F.-K. Shiah, 2003. Distributions, stoichiometric patterns and cross-shelf exports of dissolved organic matter in the East China Sea. *Deep-Sea Research II* **50**, 1127-1145.
- Jan, S., S.-Y. Chao, 2003. Seasonal variation of volume transport in the major inflow region of the Taiwan Strait: the Penghu Channel. *Deep-Sea Research II* **50**, 1117-1126.
- Liang, W.-D., T.-Y. Tang, Y.-J. Yang, M.-T. Ko, W.-S. Chuang, 2003. Upper-ocean currents around Taiwan. *Deep-Sea Research II* **50**, 1085-1105.
- Murray, J. W., J. Downs, S. Strom, C.-L. Wei, and H. W. Jannasch, 1989. Nutrient assimilation, export production and  $^{234}\text{Th}$  scavenging in the Eastern Equatorial Pacific. *Deep-Sea Research* **36**, 1471-1489.
- Radakovitch, O, M. Frignani, S. Giuliani and R. Montanari, 2003. Temporal variations of dissolved and particulate  $^{234}\text{Th}$  at a coastal station of the northern Adriatic Sea. *Estuarine, Coastal and Shelf Sciences* **58**, 813-824.
- Savoie, N., C. Benitez-Nelson, A. B. Burd, J. K. Cochran, M. Charette, K. O. Buesseler, G. A. Jackson, M. Roy-Barman, S. Schmidt, M. Elskens, 2006.  $^{234}\text{Th}$  sorption and export models in the water column: A review. *Marine Chemistry* **100**, 234-249.

- Tung, C.-H., 2007. Pigments distribution in coastal surface waters off Taiwan, M.S. thesis, National Taiwan University, pp65.
- Wei, C.-L. and C.-C. Hung, 1992. Spatial variation of  $^{234}\text{Th}$  scavenging in the surface water of the Bashi Channel and the Luzon Strait. *Journal of Oceanography* **48**, 427-437.
- Wei, C.-L. and J. W. Murray, 1992. Temporal variation of  $^{234}\text{Th}$  activity in the water column of Dabob Bay: Particle scavenging. *Limnology and Oceanography* **37**, 296-314.
- Weinstein S. E. and S. B. Moran, 2005. Vertical flux of particulate Al, Fe, Pb, and Ba from the upper ocean estimated from  $^{234}\text{Th}/^{238}\text{U}$  disequilibria. *Deep-Sea Research I* **52**, 1477-1488
- Wyrtki, K., 1961. Physical oceanography of the southeast Asia waters. Scientific results of marine investigations of the South China Sea and Gulf of Thailand. 1959-1961, Naga Report, 195pp.
- Zaneveld, J.R.V., 1994. Optical closure: from theory to measurement. In: Spinrad, R. W., K. L. Carder, and M. J. Perry (Eds.), *Ocean Optics*. Oxford Monographs on Geology and Geophysics, No. 25. Oxford University Press, Oxford, pp. 59-72.

Table 1. Temperature, salinity, concentration of total suspended matter (TSM), dissolved (DTh) and particulate (PTh)  $^{234}\text{Th}$  activities, and particulate organic carbon concentration obtained from the surface water of the Taiwan Strait. Standard deviations of DTh and PTh are based on propagated counting error ( $1\sigma$ ).

Station	Longitude (°E)	Latitude (°N)	T (°C)	S (psu)	TSM (mg/L)	DTh (dpm/L)	PTh (dpm/L)	POC ( $\mu\text{M}$ )
1	120.00	22.01	27.83	34.266	0.30	1.39 ± 0.04	0.15 ± 0.01	-
2	119.50	22.00	27.44	34.154	0.21	1.95 ± 0.05	0.16 ± 0.01	-
3	119.50	21.50	27.49	34.145	0.22	1.47 ± 0.05	0.28 ± 0.02	-
4	120.00	21.50	28.20	34.122	0.20	0.87 ± 0.02	0.16 ± 0.01	-
5	120.50	21.50	28.89	33.983	0.20	0.97 ± 0.03	0.18 ± 0.01	-
6	120.50	22.00	28.42	34.280	0.16	1.52 ± 0.03	0.11 ± 0.01	-
7	120.00	23.00	28.49	33.982	0.23	1.93 ± 0.00	0.24 ± 0.02	4.5
8	119.75	23.00	27.49	34.311	0.76	0.18 ± 0.02	0.60 ± 0.02	3.6
9	119.50	23.00	27.27	34.167	1.59	0.54 ± 0.01	0.46 ± 0.03	6.2
10	119.25	23.00	26.09	34.273	1.97	0.38 ± 0.01	0.42 ± 0.02	10.7
11	118.71	23.25	25.16	34.144	1.42	0.22 ± 0.02	0.34 ± 0.02	10.1
12	118.00	23.50	24.32	33.766	0.89	0.36 ± 0.06	0.46 ± 0.01	10.9
13	118.50	23.50	24.69	34.072	1.12	0.61 ± 0.01	0.45 ± 0.03	8.6
14	119.00	23.50	25.59	34.165	9.96	0.12 ± 0.01	0.30 ± 0.02	9.0
15	119.50	23.50	26.01	34.122	3.20	0.21 ± 0.01	0.45 ± 0.02	7.6
16	120.00	23.50	26.19	34.358	0.79	0.26 ± 0.01	0.65 ± 0.02	17.1
17	120.00	24.00	27.73	34.093	0.73	0.46 ± 0.01	0.39 ± 0.02	6.9
18	119.50	24.00	25.96	34.198	4.58	0.17 ± 0.00	0.45 ± 0.01	6.2
19	119.00	24.00	24.59	34.208	0.73	0.46 ± 0.01	0.39 ± 0.02	9.4
20	118.50	24.33	22.33	31.933	4.58	0.17 ± 0.06	0.45 ± 0.01	16.9
21	119.00	24.50	23.75	34.101	1.07	0.05 ± 0.01	0.23 ± 0.02	7.6
22	119.50	24.50	26.02	34.141	0.78	0.04 ± 0.01	0.27 ± 0.02	7.1
23	119.50	25.00	21.39	32.509	5.28	0.73 ± 0.00	0.22 ± 0.01	15.3
24	120.00	25.00	24.66	34.198	1.65	0.04 ± 0.01	0.28 ± 0.02	8.6
25	120.00	24.49	26.94	34.168	1.12	0.33 ± 0.01	0.34 ± 0.02	8.4
26	120.50	24.50	28.06	34.010	2.69	0.12 ± 0.02	0.30 ± 0.02	7.7
27	120.67	25.00	25.07	34.207	0.98	0.59 ± 0.01	0.30 ± 0.01	6.8
28	120.50	25.50	21.33	31.513	1.24	0.14 ± 0.01	0.15 ± 0.01	22.6
29	121.00	25.50	24.87	34.257	0.64	0.16 ± 0.00	0.21 ± 0.02	7.2
30	121.50	25.50	26.20	34.203	1.43	0.13 ± 0.01	0.34 ± 0.01	6.1
31	120.00	26.00	20.71	26.807	1.90	0.13 ± 0.00	0.14 ± 0.02	19.3

32	117.00	22.50	25.32	34.041	0.97	$0.33 \pm 0.01$	$0.43 \pm 0.02$	-
33	117.50	22.50	26.16	34.054	0.68	$0.28 \pm 0.01$	$0.42 \pm 0.02$	-
34	118.00	22.50	26.34	34.143	0.35	$0.32 \pm 0.01$	$0.46 \pm 0.03$	-
35	118.50	22.50	26.47	34.141	0.47	$0.34 \pm 0.01$	$0.43 \pm 0.03$	-
36	119.00	22.50	27.15	34.182	0.20	$0.67 \pm 0.02$	$0.21 \pm 0.01$	-
37	119.50	22.50	27.29	34.166	0.16	$1.58 \pm 0.04$	$0.41 \pm 0.03$	-
38	120.00	22.50	28.44	34.013	0.17	$1.36 \pm 0.05$	$0.47 \pm 0.03$	-

---

---

Table 2. Parameters used and the results of the advective-scavenging-removal model for the five domains in the Taiwan Strait.

<b>Box</b>	<b>DTh</b> <b>(dpm/L)</b>	<b>PTh</b> <b>(dpm/L)</b>	<b>V<sub>in</sub></b> <b>(cm/s)</b>	<b>V<sub>out</sub></b> <b>(cm/s)</b>	<b>J</b> <b>dpm/m<sup>3</sup>/day</b>	<b>P</b> <b>dpm/m<sup>3</sup>/day</b>	<b>τ<sub>D</sub></b> <b>day</b>	<b>τ<sub>P</sub></b> <b>day</b>	<b>POC/PTh</b> <b>mmol/dpm</b>	<b>P<sub>c</sub></b> <b>mmol/m<sup>3</sup>/d</b>	<b>τ<sub>c</sub></b> <b>day</b>
<b>I</b>	1.59 ± 0.23	0.26 ± 0.13	65.0	33.7	91 ± 61	138 ± 77	18 ± 12	2 ± 1	13.5 ± 8.2	1.9 ± 1.5	3 ± 2
<b>II</b>	0.36 ± 0.14	0.39 ± 0.09	9.2	21.1	66 ± 31	24 ± 35	6 ± 3	16 ± 24	23.7 ± 4.6	0.6 ± 0.8	17 ± 26
<b>III</b>	0.32 ± 0.16	0.51 ± 0.09	33.7	38.9	520 ± 133	381 ± 150	1 ± 0	1 ± 1	18.1 ± 8.9	6.9 ± 3.5	1 ± 1
<b>IV</b>	0.06 ± 0.04	0.27 ± 0.03	38.9	43.9	175 ± 61	224 ± 76	0 ± 0	1 ± 0	29.4 ± 13.1	6.6 ± 3.7	1 ± 1
<b>V</b>	0.14 ± 0.02	0.21 ± 0.09	43.9	31.6	57 ± 9	76 ± 20	3 ± 1	3 ± 1	66.1 ± 49.7	5.0 ± 4.0	3 ± 3



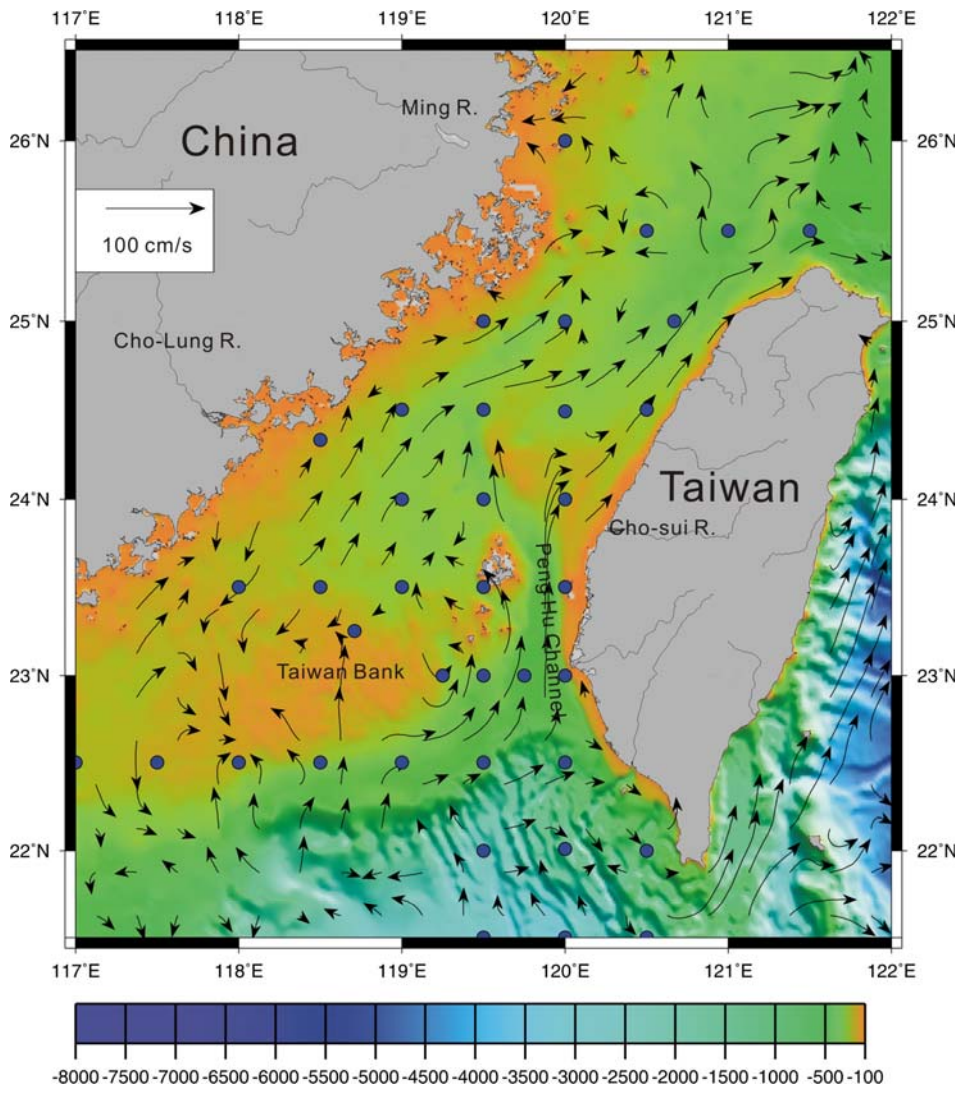


Figure 1

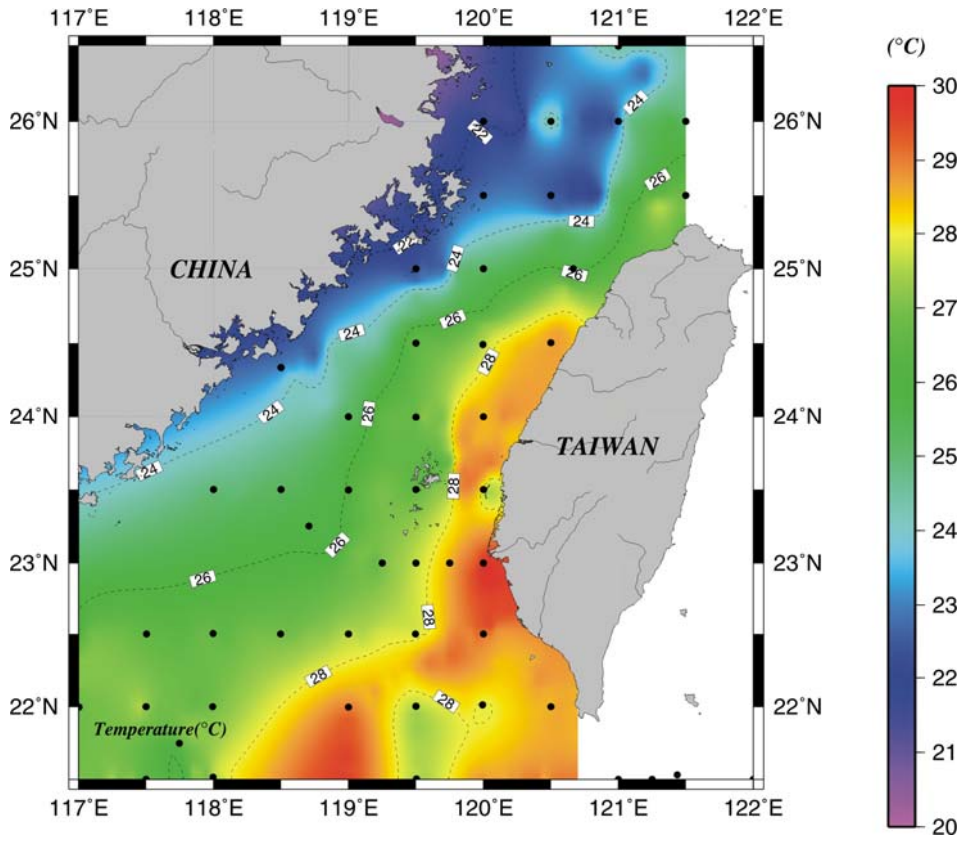


Figure 2

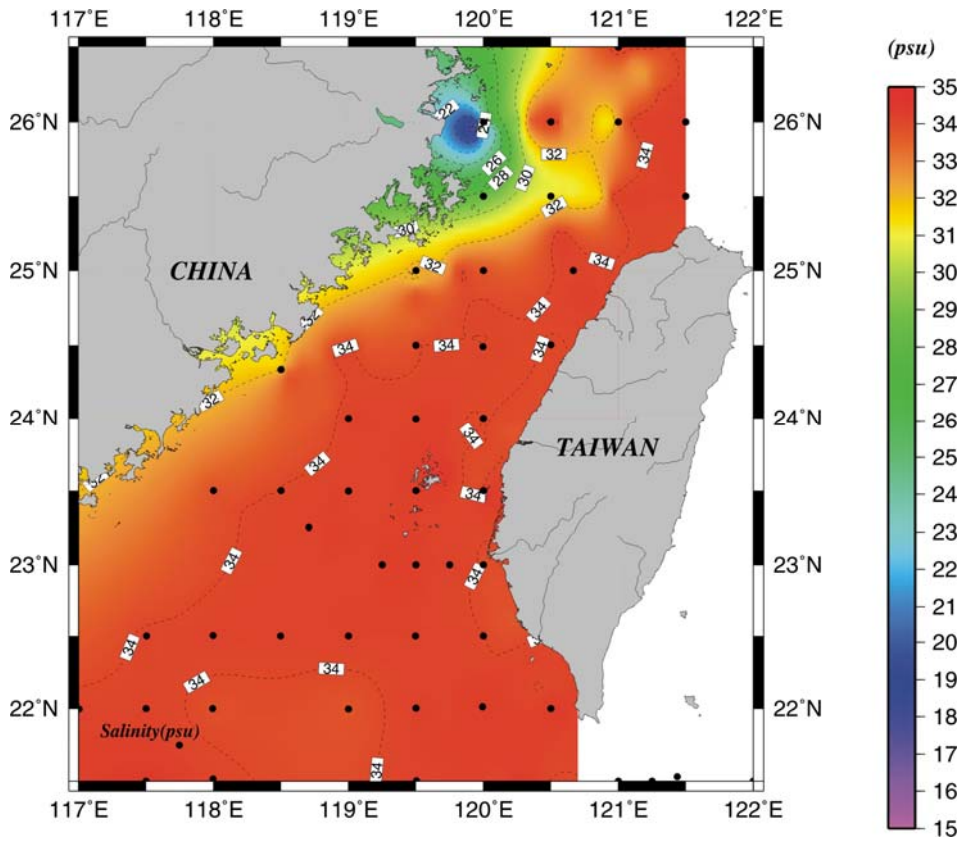


Figure 3

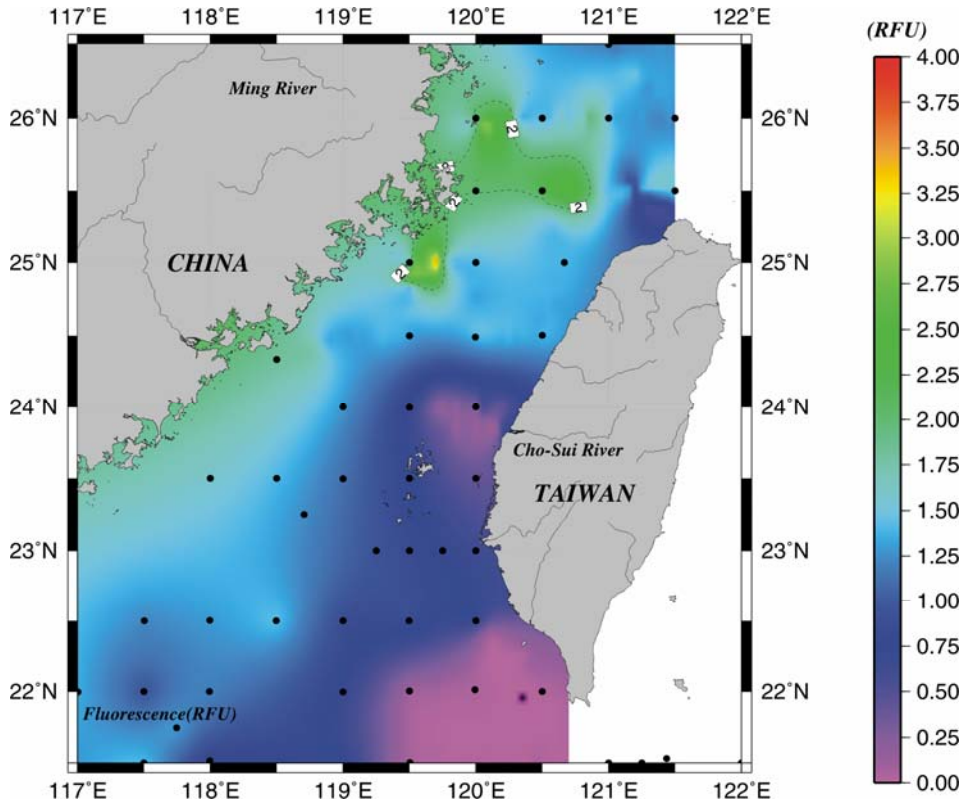


Figure 4

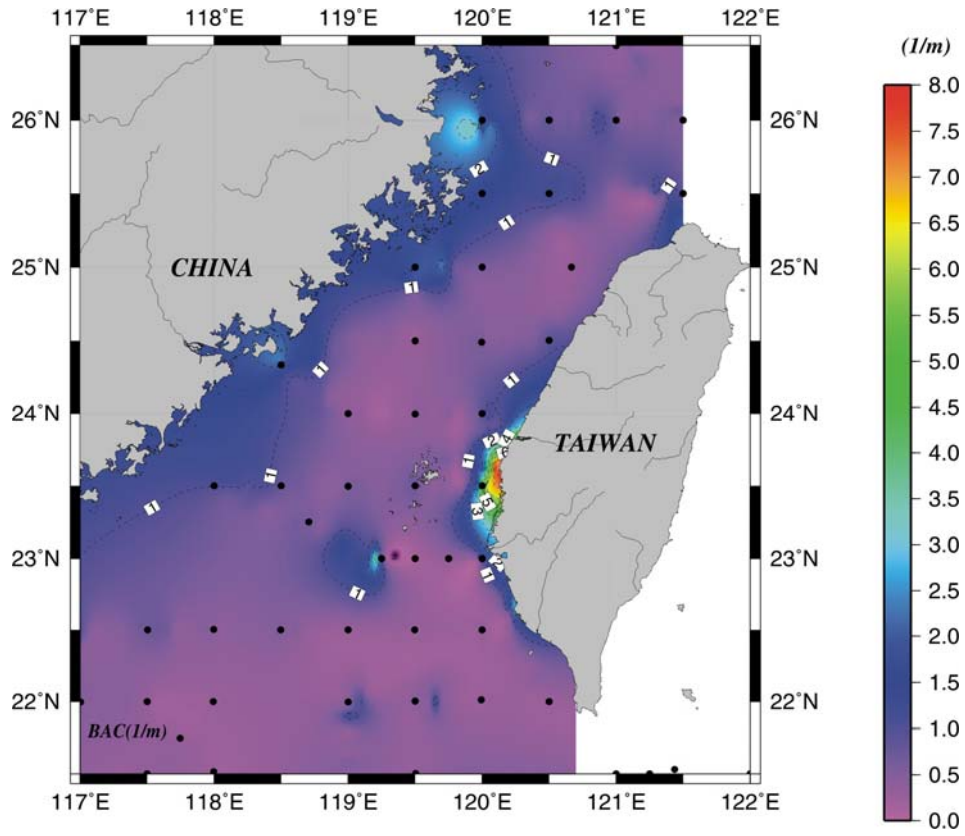


Figure 5

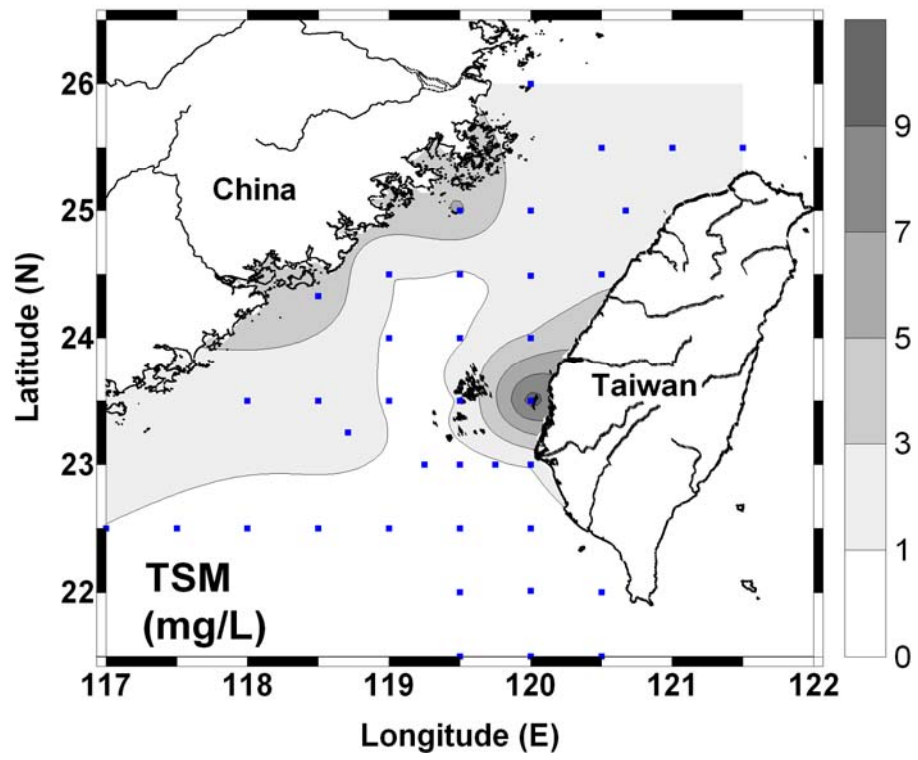


Figure 6

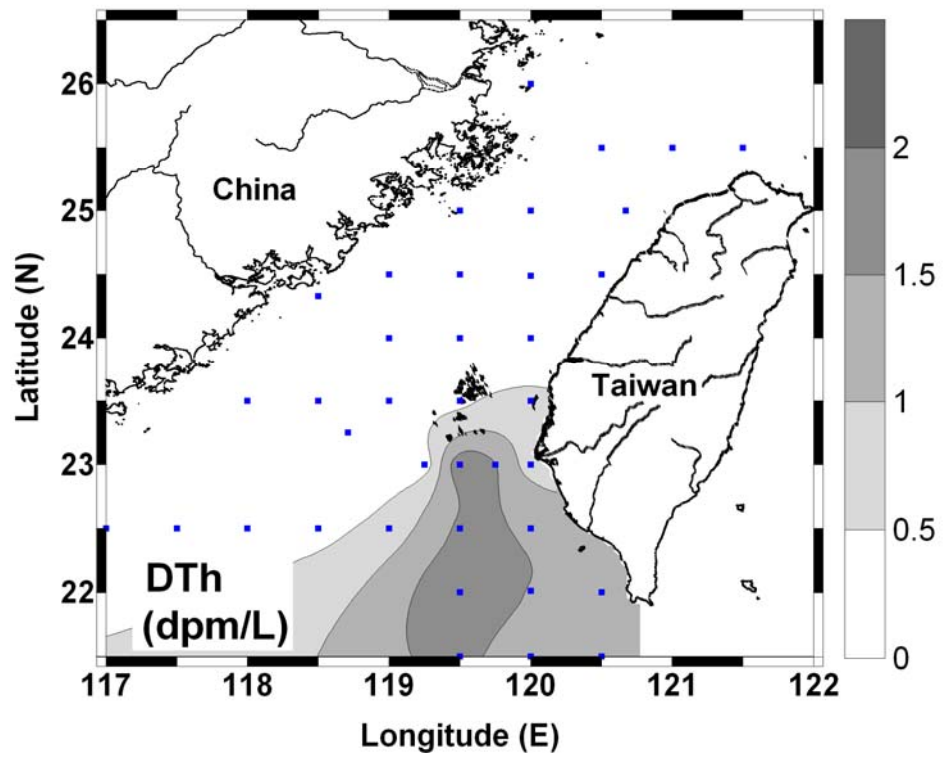


Figure 7



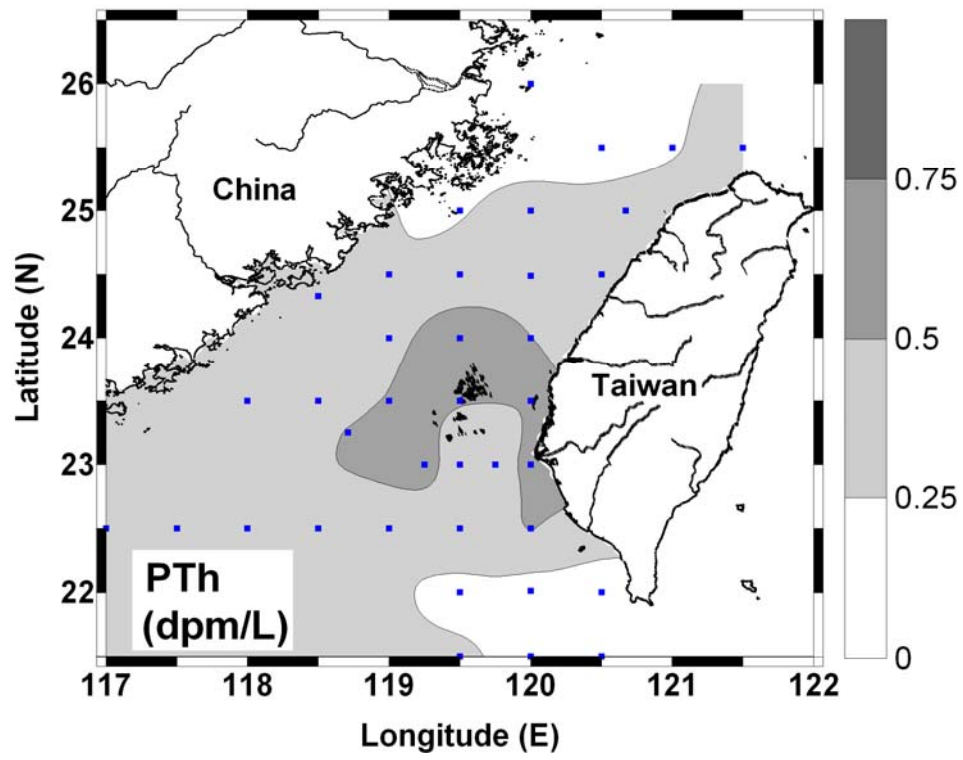


Figure 8



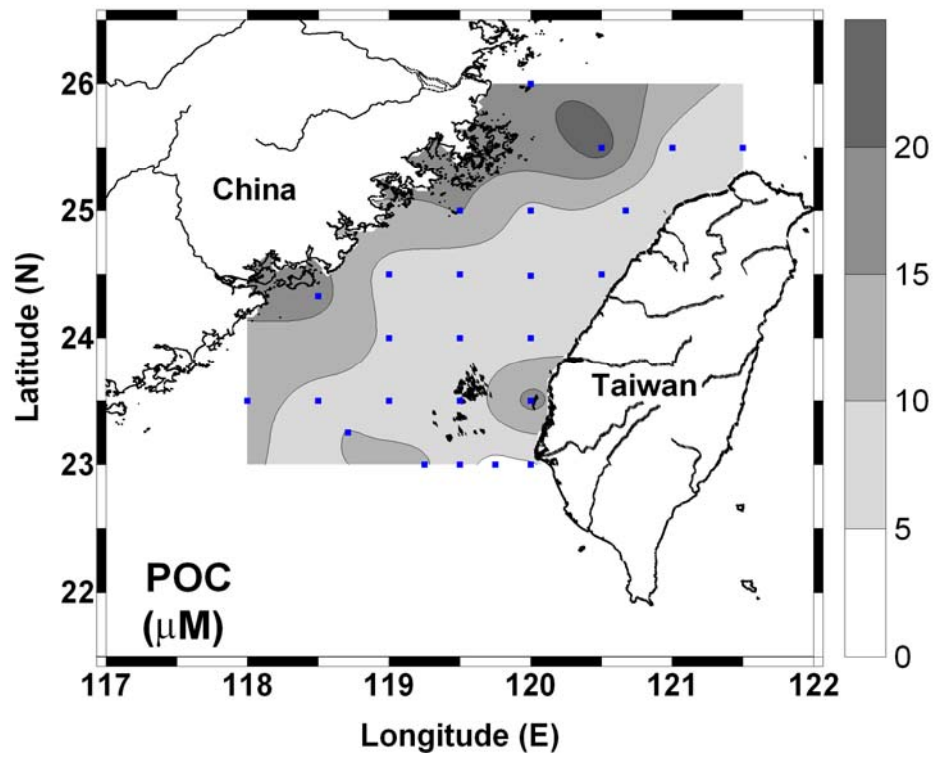


Figure 9

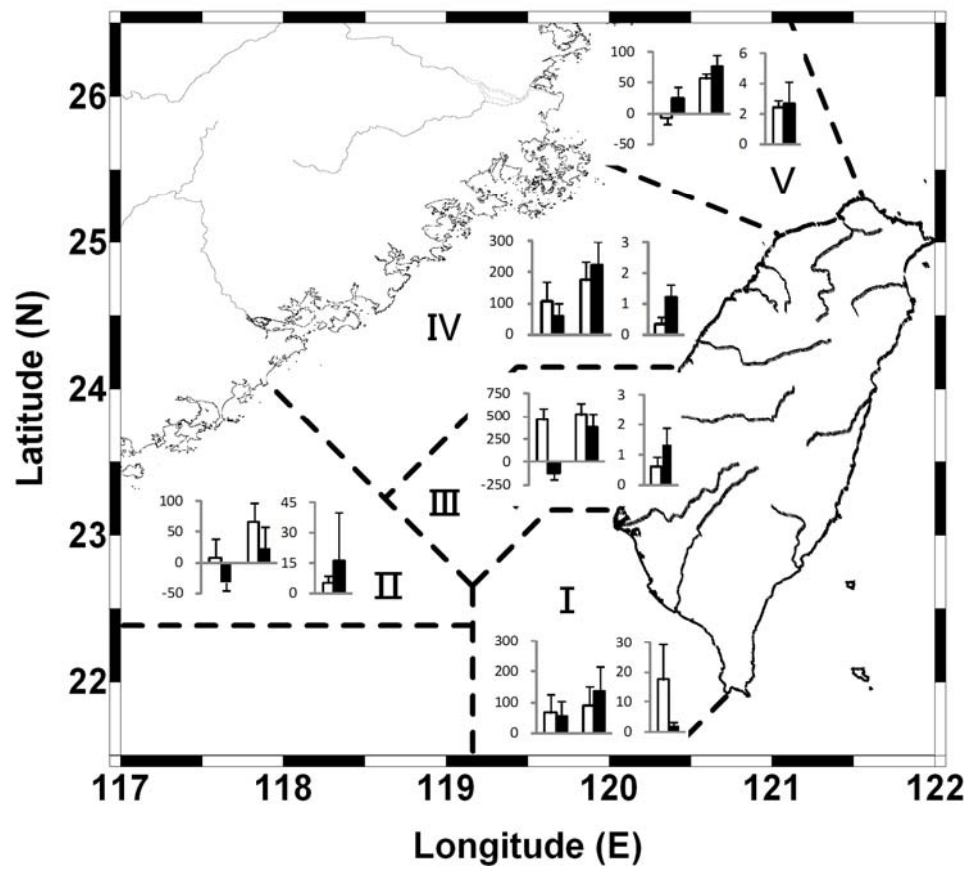


Figure 10

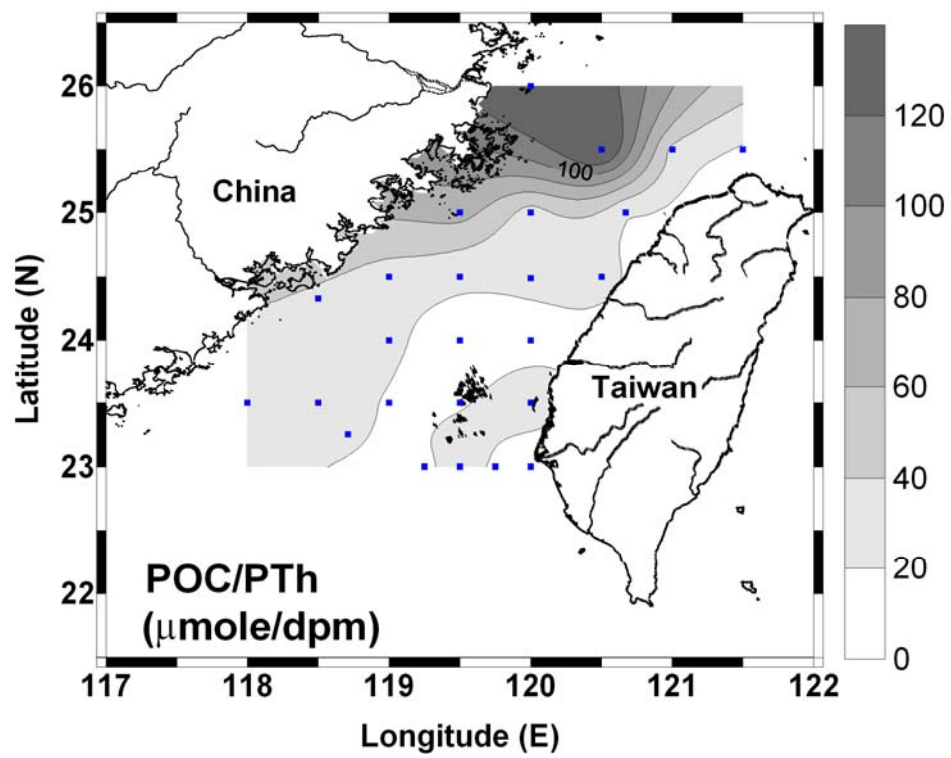


Figure 11